Heat capacity and thermal conductivity of hexagonal pyrolytic boron nitride

E. K. Sichel, R. E. Miller, M. S. Abrahams, and C. J. Buiocchi
RCA Laboratories, Princeton, New Jersey 08540
(Received 26 January 1976)

We have measured the heat capacity and thermal conductivity of the layered material hexagonal pyrolytic boron nitride from 2 to 10 K by a pulse-heating technique. The thermal conductivity has also been determined by a steady-state technique from 1.5 to 350 K. At low temperatures, the heat capacity has a T^3 dependence and the thermal conductivity a $T^{2.4}$ dependence. Crystallite size was found from transmission electron micrographs. The influence of dislocations on the thermal conductivity is discussed.

I. INTRODUCTION

The hexagonal layer structures graphite and boron nitride (BN) are isomorphic. Carbon lies between boron and nitrogen in the Periodic Table. The lattice constants are similar, i.e., for BN, $a_0 = 2.504$ Å, $c_0 = 6.661$ Å and for graphite $a_0 = 2.456$ Å and $c_0 = 6.696$ Å. The differences between graphite and BN are also notable. BN is a whitish insulating material and looks much like mica. Graphite is black and an electrical conductor.

Both materials are strongly bonded within an atomic layer, but bonding between layers is weak, of the Van der Waals type. The anisotropic character of these layer structures has inspired many studies of the lattice heat capacity.[1-4] In both BN (Ref. 4) and graphite[3] the lattice heat capacity varies as T^2 in some temperature region above 13 K. This has been interpreted as being a consequence of anisotropic lattice forces.[5] At sufficiently low temperatures, below 10 K, the lattice heat capacity is expected to have a T^3 dependence.[5,6] This has been observed[1] in natural graphite (but not pyrolytic graphite[2]) below 10 K. In the case of BN, no low-temperature ($T < 20$ K) data have been reported.

This paper is an experimental study of the low-temperature heat capacity and thermal conductivity of BN. We report on the crystal characteristics of our BN sample in Sec. II and our experimental techniques for measuring heat capacity and thermal conductivity in Sec. III. Our results are presented and discussed in Sec. IV.

II. SAMPLE CHARACTERISTICS

The specimen was pyrolytic compression annealed BN prepared in a way described by Moore.[7] Specimen dimensions were $X = 5.1$ cm, $Y = 0.69$ cm, $Z = 0.11$ cm. The c axis was in the Z direction and the XY plane was the basal plane. The crystal structure of BN is shown in Fig. 1.

X-ray studies revealed that the sample consisted of small crystallites which are platelets in the basal plane. Platelet thickness along the c axis was determined from the line broadening. The mosaic spread in c axis alignment was determined from the full width at half-maximum of the (00·2) Cu $K\alpha$ reflection from BN. Some sample parameters are given below:

Theoretical density[7]:	2.28 g/cm^3,
Density determined by displacement method:	2.18 g/cm^3,
FWHM spread in c-axis alignment:	2°,
Crystallite thickness along c-axis:	500–1000 Å.

Platelet dimensions in the basal plane were determined from transmission electron micrographs of thin samples cleaved from the specimen. The thin samples were coated with carbon to prevent charging of the BN in the electron beam.

A Philips 300 electron microscope operating at 100 kV was used for these studies. At low magnification, individual crystallites can be distinguished by nature of the abrupt contrast changes occurring across differently oriented crystallites. The crystallite diameters are typically 6200 ± 2900 Å.

At higher magnification in Fig. 2, a clear example of a crystallite (diameter $\simeq 10^4$ Å) is seen. The crystallite is made visible here by moiré fringe contrast. Since the fringes are parallel to $\vec{g}$, the operative reciprocal-lattice vector, the moiré pattern is of the rotational type.[8] From

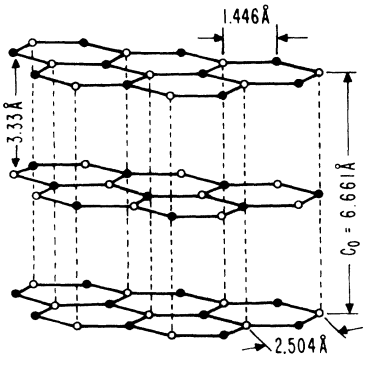

HEXAGONAL BORON NITRIDE

FIG. 1. Structure of hexagonal boron nitride.

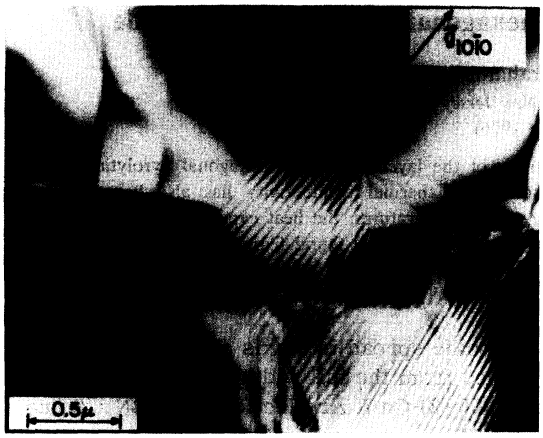

FIG. 2. Transmission electron micrograph of boron nitride. Dark field, $\vec{g} = [10\bar{1}0]$ with several closely spaced spots included in aperture.

the observed fringe spacing ($\simeq 405$ Å), a rotational misalignment of 0.31° is obtained for the two overlapping crystallites giving rise to the moiré pattern.

Figure 3(a) shows a typical diffraction pattern for BN, with the thin specimen in a nearly perfect basal-plane orientation. In addition to the primary diffraction spots (for example, $\langle 10\bar{1}0\rangle$ and $\langle 11\bar{2}0\rangle$), many secondary spots are visible. These probably arise from multiple double diffraction[8] from more than two overlapping crystallites. Figure 3(b) is an (0001) diffraction pattern obtained from a cleaved sample of pyrolytic graphite. The similarity of Figs. 3(a) and 3(b) is evident as expected since BN and C have the same crystal structure and almost identical lattice constants.

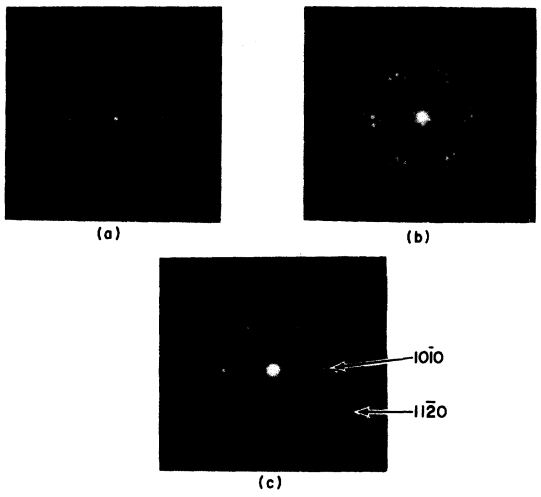

FIG. 3. Diffraction pattern of (a) boron nitride, (b) and (c) pyrolytic graphite. (0001) foil orientation. Note decrease in spot density in (c) relative to (b) as sample is traversed to thinner region.

However, as the graphite sample was traversed to a thinner region, the diffraction pattern in Fig. 3(c) was obtained. It is seen that the plethora of diffraction spots present in Fig. 3(b) is considerably reduced, thus supporting our belief that double diffraction events involving several crystallites are responsible for diffractions patterns such as that in Fig. 3(a). It was not possible to cleave a sufficiently thin BN sample to obtain a simple diffraction pattern.

It is also noted that x-ray diffractometry failed to reveal the presence of polytypes or superstructure in the BN.

III. EXPERIMENTAL TECHNIQUES: HEAT CAPACITY AND THERMAL CONDUCTIVITY

We used a pulse technique to determine the heat capacity. The apparatus is shown in Fig. 4. A heater *H*, 2 mg, was fastened with General Electric 7031 varnish to one end of the specimen *S*. The heater covered the *YZ* plane. We used an evaporated constantan heater on a thin insulating substrate, sold commercially as a strain gauge. The voltage leads were 0.008-cm-diam manganin wire to minimize the heat leak. The other end of the specimen was clamped in a copper holder, part of a copper heat sink. Indium and Apiezon grease were placed between the specimen and the copper and the clamp was tightened until the indium flowed. A single $\frac{1}{8}$-W Allen Bradley thermometer *T* was sanded flat and glued midway between the heater and the heat sink. The carbon thermometer was calibrated *in situ* against a germanium thermomenter in the presence of exchange gas. The carbon thermometer had a mass of about 5 mg. The specimen, approximately 190 mg, was enclosed in a copper vacuum can. We estimate that the heat capacity of the addenda was less than 5% of the total heat capacity at the temperatures studied.

The heater was energized with either a square voltage pulse or a capacitor discharge; the temperature response of the sample was determined by monitoring the thermometer response as a function of time. The pulse width was at least an order of magnitude shorter than the time for a discernible temperature change to occur at the

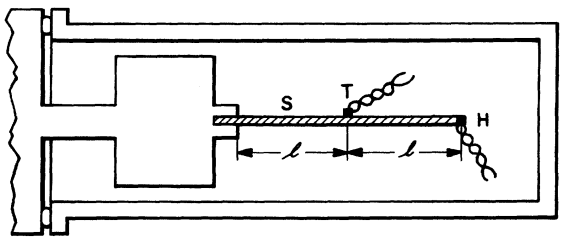

FIG. 4. Heat capacity apparatus. *H*, heater; *S*, specimen; *T*, thermometer.

thermometer. The resistance of the thermometer as a function of time was displayed on an oscilloscope. Temperature-versus-time graphs were generated from the oscilloscope traces.

The heat capacity C was determined in two ways as described below. C may be found from the maximum temperature excursion ΔT_m if the sample can be approximated by an infinitely long slab and the heat pulse by a δ function.[9] The heat capacity of the heater and thermometer must be negligible. The heat flow is assumed to be one dimensional. Then, the heat capacity per unit volume is given by

$$C = 2Q/(\Delta T_m)(2\pi e)^{1/2} lA \,, \tag{1}$$

where Q is the energy in the pulse, ΔT_m is the maximum temperature excursion at a distance l from the heater, and A is the cross-sectional area of the specimen. We compared with Eq. (1) the exact solution for one-dimensional heat flow in a finite sample under our experimental conditions. The difference was negligible.

The thermal conductivity K can be determined from the diffusivity D, where $D = l^2/2t_m$, where t_m is the time at which ΔT_m occurs. The pulse is applied at $t = 0$. The thermal conductivity is given by $K = DC$.

Another technique[10] determines the heat capacity and thermal conductivity from the area under the ΔT-vs-time (t) curve. Two quantities are computed, f_0 and f_1, where

$$f_0 = \int_0^\infty \Delta T(t)\, dt \tag{2}$$

and

$$f_1 = \int_0^\infty \Delta T(t) t\, dt \,. \tag{3}$$

If the heat capacity of the heater and thermometer can be neglected, the sample heat capacity per unit volume is given by

$$C = Qf_1/Alf_0^2 \,. \tag{4}$$

The thermal conductivity is given by

$$K = Ql/Af_0 \,. \tag{5}$$

The heat pulse is assumed to be a δ function, but infinite sample length is not assumed.

We obtained the same results for the heat capacity using either Eq. (1) or (4). As a further check, we compared the values of thermal conductivity determined by Eq. (5) by the pulse technique with the values determined from the diffusivity and these in turn we compared with values previously reported[11] by us for the same sample in a conventional steady-state thermal conductivity experiment. The thermal conductivity results are shown in Fig. 5. At low temperatures, K varies as $T^{2.4\pm0.1}$. Our room-temperature thermal conductivity values for this sample are higher than those reported by Simpson and Stuckes,[12] and it has been shown[11,12] that the thermal conductivity of BN is a sensitive function of crystal perfection.

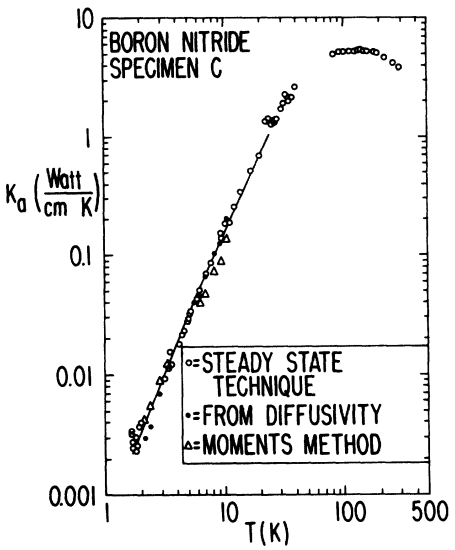

FIG. 5. Thermal conductivity of BN as a function of temperature. Open circles, steady-state technique; triangles, pulse technique, moments method; dots, pulse technique, from diffusivity; solid line, theoretical fit for boundary and dislocation scattering.

As a final check on our technique we measured the heat capacity of a commercial pyrolytic graphite sample (type HPG, Union Carbide Corp., density 2.2 g/cm^3) from 2 to 5 K with our pulse-heating technique. We used the same type of heater and thermometer used with the BN sample and the same sample configuration. Our data are in excellent agreement in magnitude and slope with those of Van der Hoeven and Keesom[2] for pyrolytic graphite at the overlap point of the data.

IV. RESULTS AND DISCUSSION

The heat capacity of BN as a function of temperature is shown in Fig. 6 along with the higher-temperature data of Dworkin *et al.*[4] It does not appear as if the data would overlap smoothly with our results. We do not know the origin of this difference. Our data follow a T^3 dependence in this temperature range with a Debye parameter θ_D of 323 K. Dworkin *et al.*[4] have reported that at higher temperature, the heat capacity of BN varies as T^2. The same effect has been observed[1] in the lattice heat capacity of graphites. Krumhansl and Brooks[5] have shown that at low temperatures and low-phonon frequencies the density of lattice vibrations per unit frequency range in graphite is the same as for a three-dimensional system and the heat capacity should vary as T^3.

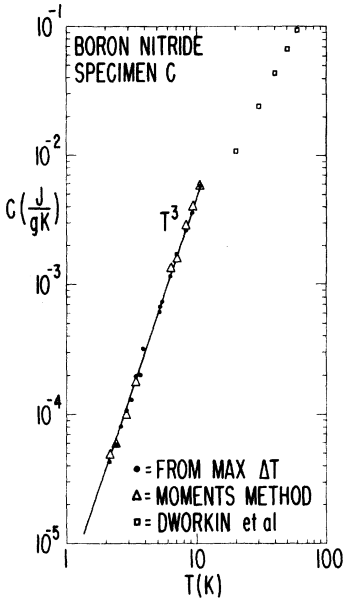

FIG. 6. Heat capacity of BN as a function of temperature. The squares are data of Dworkin *et al.* (Ref. 4).

At some higher frequency, the surface of constant phonon frequency in momentum space begins to touch the Brillouin zone. In graphite and hexagonal boron nitride the Brillouin zones form a flattened disklike volume, with a hexagonal perimeter. Krumhansl and Brooks[5] have shown that when the surfaces of constant phonon frequency begin to touch the zone boundaries, their surfaces become truncated at the contact points and the density of lattice vibrations per unit frequency range grows more slowly as the frequency increases. This results in a region of T^2 dependence of the lattice heat capacity. Eventually, at high temperatures, the heat capacity approaches the Dulong-Petit value.

It is notable that the heat capacity and thermal conductivity of hexagonal boron nitride do not have the same temperature dependence below 10 K; $K \propto T^{2.4}$ and $C \propto T^3$. If scattering of phonons off the crystallite boundaries were the only important limitation of the thermal conductivity, then

$$K = \tfrac{1}{3} C v l \,, \tag{6}$$

where K is the thermal conductivity, C is the heat capacity per unit volume, v is the average sound velocity, and l is the average crystallite size. The heat capacity and thermal conductivity would have the same temperature dependence in the boundary scattering regime. The most likely additional phonon scattering mechanism is phonon-dislocation scattering. Acting alone, phonon-dislocation scattering would give a T^2 dependence to the thermal conductivity at low temperatures.[13]

Acting in concert with boundary scattering, the dislocation scattering could result in the $T^{2.4}$ dependence we have observed. The thermal conductivity of an isotropic solid at low temperatures can be expressed[13,14] as

$$K = \frac{4Lk^4T^3\pi}{h^3}\int \frac{e^x x^4\,dx}{(e^x-1)^2[(2vxTDLk\pi/h)+v^2]} \,, \tag{7}$$

where L is the phonon mean free path for boundary scattering, v is the average sound velocity, and

$$D = 2.3\gamma^2 b^2 N_d \,. \tag{8}$$

This dislocation scattering term has been studied by Ackerman[15] and Klaffky *et al.*[14] γ is the Grüneisen constant, b is the Burgers vector for dislocations, and N_d is the dislocation density.

Equation (7) is not the best expression to use for anisotropic materials like graphite and boron nitride. An estimate of the anisotropy is given by the ratio $L_a : L_c$ of a typical crystallite. For our specimen, $L_a \sim 7500$ Å and $L_c \sim 750$ Å; the anisotropy ratio $L_a : L_c$ is 10 : 1. Slack[16] has modified the thermal conductivity integral for the case of graphite at low temperature for boundary scattering only. He defined an average sound velocity $\bar{v}_0$ averaged over different polar angles θ. We do not know of any theoretical work treating the effect of crystal anisotropy on phonon-dislocation scattering; therefore, as a first approximation, we have fit our data to Eq. (7), substituting Slack's computed value of $\bar{v}_0$ for v. This approach neglects the crystal anisotropy except in so far as it influences the sound velocity.

Rewriting Eq. (7) as

$$K_a = T^3 \int_0^{x_c} \frac{e^x x^4\,dx}{(\alpha T x+\beta)(e^x-1)^2} \,, \tag{9}$$

we can fit our data from 1.5 to 25 K to an integral of this form where $x_c = 20$, $\alpha = 3.325\times10^{-4}$ cm sec K^3/erg, and $\beta = 3.37\times10^{-3}$ cm K^4 sec/erg. If we choose $\bar{v}_0 = 2.9\times10^5$ cm/sec, the value computed by Slack for graphite, we find $L \simeq 15.9$ μm. This is larger, by more than an order of magnitude, than a typical crystallite dimension. We conclude that the individual crystallites are not the origin of phonon-boundary scattering here. If we *assume* $b \sim 3\times10^{-8}$ cm and $\gamma \sim 1.5$, then we compute $N_d \sim 2.9\times10^{10}$ cm^{-2} using our value of β and Eqs. (7) and (8).

We now discuss the dislocation density. The strain resulting from the rotational misalignment between neighboring crystallites ($\theta \sim 0.3°$) can be accommodated by the formation of a dislocation boundary[17] in which the spacing for small θ is

$$D_0 \sim b/\theta \,, \tag{10}$$

where b is the Burgers vector and θ is the angular difference in orientation between two grains. If we assume $b \sim 3\times10^{-8}$ cm and $\theta \sim 0.3^\circ = 5.2\times10^{-3}$ rad, then $D_0 \sim 0.58\times10^{-5}$ cm. Strictly, this holds for edge dislocations, but we assume that the density of edge dislocations is the same order of magnitude as the total dislocation density. We have found $N_d \sim 2.9\times10^{10}$ cm^{-2} from the thermal conductivity data. If we assume a uniform distribution of dislocations, this implies that the spacing between dislocations is $\sim 0.58\times10^{-5}$ cm. In view of the simplifying approximations used in these calculations, the order of magnitude agreement in the dislocation spacing is striking.

From studying the temperature dependence of the heat capacity and thermal conductivity of hexagonal BN, we conclude that boundary scattering and dislocation scattering limit the low-temperature thermal conductivity. We use an average value of the sound velocity computed by Slack[16] for graphite. We find that the individual crystallites do not determine the boundary scattering mean free path. This is probably a consequence of the small degree ($\sim 0.3^\circ$) of rotational misalignment between neighboring crystallites. The crystallites limit the thermal conductivity through dislocation scattering because dislocation boundaries are formed as a result of the strain due to the rotational misalignment between neighboring crystallites. The dislocation spacing estimated from the thermal conductivity data is consistent with this idea.

ACKNOWLEDGMENTS

The boron-nitride crystals used in this study were kindly supplied by A. W. Moore of Union Carbide Corp. We are grateful to A. W. Moore for suggesting that a comparison of the diffraction patterns of BN and graphite would be instructive. R. Smith (RCA) did the x-ray analysis of the specimen. We had numerous helpful discussions with L. J. Vieland, R. W. Cohen, and J. Blanc.

[1]W. DeSorbo and G. E. Nichols, J. Phys. Chem. Solids 6, 352 (1958).
[2]B. J. C. van der Hoeven, Jr. and P. H. Keesom, Phys. Rev. 130, 1318 (1963).
[3]W. DeSorbo and W. W. Tyler, J. Chem. Phys. 21, 1660 (1953).
[4]A. S. Dworkin, D. J. Sasmor, and E. R. Van Artsdalen, J. Chem. Phys. 22, 837 (1954).
[5]J. Krumhansl and H. Brooks, J. Chem. Phys. 21, 1663 (1953).
[6]P. G. Klemens, Australian J. Phys. 6, 405 (1953).
[7]A. W. Moore, Nature 221, 1133 (1969).
[8]P. B. Hirsch, A. Howie, R. B. Nicholson, D. W. Pashley, and M. J. Whelan, *Electron Microscopy of Thin Crystals* (Butterworth, Washington, D. C., 1965), p. 357.
[9]B. Bertman, D. C. Heberlein, D. J. Sandiford, L. Shen, and R. R. Wagner, Cryogenics 10, 326 (1970). The expression for C in this paper is in error by a factor of 2 which has been corrected in Eq. (1).
[10]S. Alterovitz, A. Deutscher, and M. Gershenson, Appl. Phys. 5, 329 (1975).
[11]E. K. Sichel and R. E. Miller, *Proceedings of the Fourteenth International Conference on Thermal Conductivity, June* 1975 (Plenum, New York, to be published).
[12]A. Simpson and A. D. Stuckes, J. Phys. C 4, 1710 (1971).
[13]P. G. Klemens, *Encyclopedia of Physics*, edited by S. Flügge (Springer-Verlag, Berlin, 1956), Vol. 14, p. 198.
[14]R. W. Klaffky, N. S. Mohan, D. H. Damon, Phys. Rev. B 11, 1297 (1975).
[15]M. W. Ackerman, Phys. Rev. B 5, 2751 (1972).
[16]G. A. Slack, Phys. Rev. 127, 694 (1962).
[17]W. T. Read, Jr., *Dislocations in Crystals* (McGraw-Hill, New York, 1953), Chap. 11.

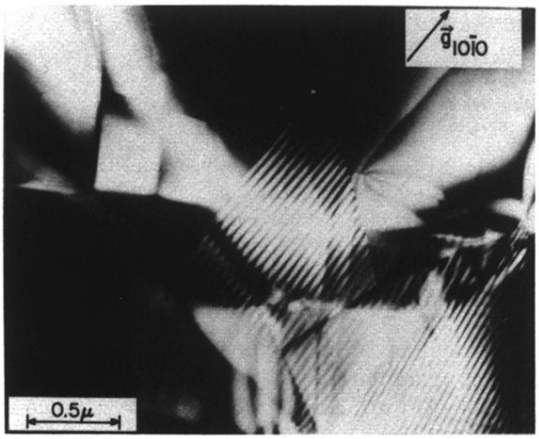

FIG. 2. Transmission electron micrograph of boron nitride. Dark field, $\vec{g} = [10\bar{1}0]$ with several closely spaced spots included in aperture.

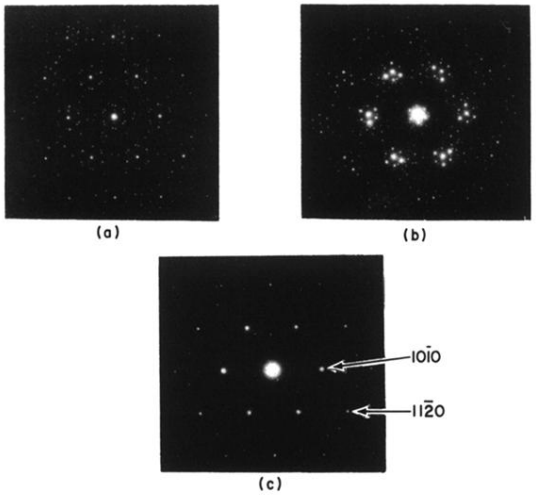

FIG. 3. Diffraction pattern of (a) boron nitride, (b) and (c) pyrolytic graphite. (0001) foil orientation. Note decrease in spot density in (c) relative to (b) as sample is traversed to thinner region.